

Minerva Access is the Institutional Repository of The University of Melbourne

Author/s:

Oskin, P; Mizuk, R; Aihara, H; Asner, DM; Atmacan, H; Aulchenko, V; Aushev, T; Ayad, R; Behera, P; Belous, K; Bennett, J; Bessner, M; Bhardwaj, V; Bhuyan, B; Bilka, T; Biswal, J; Bonvicini, G; Bozek, A; Bračko, M; Browder, TE; Campajola, M; Cao, L; Červenkov, D; Chang, P; Chekelian, V; Chen, A; Cheon, BG; Chilikin, K; Cho, HE; Cho, K; Choi, SK; Choi, Y; Choudhury, S; Cinabro, D; Cunliffe, S; De Nardo, G; Dhamija, R; Di Capua, F; Dingfelder, J; Doležal, Z; Dong, TV; Dubey, S; Eidelman, S; Epifanov, D; Ferber, T; Ferlewicz, D; Fulsom, BG; Garg, R; Gaur, V; Gabyshev, N; Garmash, A; Giri, A; Goldenzweig, P; Golob, B; Gudkova, K; Hadjivasiliou, C; Hara, T; Hartbrich, O; Hayashii, H; Hedges, MT; Hernandez Villanueva, M; Hou, WS; Hsu, CL; Iijima, T; Inami, K; Ishikawa, A; Itoh, R; Iwasaki, M; Iwasaki, Y; Jacobs, WW; Jia, S; Jin, Y; Joo, CW; Joo, KK; Kaliyar, AB; Kang, KH; Karyan, G; Kichimi, H; Kiesling, C; Kim, CH; Kim, DY; Kim, YK; Kinoshita, K; Kodyš, P; Korpar, S; Kotchetkov, D; Križan, P; Kroeger, R; Krovovny, P; Kulasiri, R; Kumar, R; Kumara, K; Kwon, YJ; Lange, JS; Lee, SC; Lewis, P; Li, CH; Li, LK; Li Gioi, L; Libby, J

Title:

Search for transitions from (4S) and (5S) to η_b (1S) and η_b (2S) with emission of an ω meson

Date:

2020-11-30

Citation:

Oskin, P., Mizuk, R., Aihara, H., Asner, D. M., Atmacan, H., Aulchenko, V., Aushev, T., Ayad, R., Behera, P., Belous, K., Bennett, J., Bessner, M., Bhardwaj, V., Bhuyan, B., Bilka, T., Biswal, J., Bonvicini, G., Bozek, A., Bračko, M., ... Libby, J. (2020). Search for transitions from (4S) and (5S) to η_b (1S) and η_b (2S) with emission of an ω meson. *Physical Review D*, 102 (9), <https://doi.org/10.1103/PhysRevD.102.092011>.

Persistent Link:

<https://hdl.handle.net/11343/273727>

License:

CC BY

Search for transitions from $\Upsilon(4S)$ and $\Upsilon(5S)$ to $\eta_b(1S)$ and $\eta_b(2S)$ with emission of an ω meson

P. Oskin⁴¹, R. Mizuk,^{41,18} H. Aihara,⁸⁴ D. M. Asner,³ H. Atmacan,⁷ V. Aulchenko,^{4,62} T. Aushev,¹⁸ R. Ayad,⁷⁷ P. Behera,²⁴ K. Belous,²⁸ J. Bennett,⁴⁹ M. Bessner,¹⁵ V. Bhardwaj,²¹ B. Bhuyan,²² T. Bilka,⁵ J. Biswal,³² G. Bonvicini,⁸⁷ A. Bozek,⁵⁹ M. Bračko,^{46,32} T. E. Browder,¹⁵ M. Campajola,^{29,54} L. Cao,² D. Červenkov,⁵ P. Chang,⁵⁸ V. Chekelian,⁴⁷ A. Chen,⁵⁶ B. G. Cheon,¹⁴ K. Chilikin,⁴¹ H. E. Cho,¹⁴ K. Cho,³⁶ S.-K. Choi,¹³ Y. Choi,⁷⁵ S. Choudhury,²³ D. Cinabro,⁸⁷ S. Cunliffe,⁸ G. De Nardo,^{29,54} R. Dhamija,²³ F. Di Capua,^{29,54} J. Dingfelder,² Z. Doležal,⁵ T. V. Dong,¹⁰ S. Dubey,¹⁵ S. Eidelman,^{4,62,41} D. Epifanov,^{4,62} T. Ferber,⁸ D. Ferlewicz,⁴⁸ B. G. Fulsom,⁶⁴ R. Garg,⁶⁵ V. Gaur,⁸⁶ N. Gabyshev,^{4,62} A. Garmash,^{4,62} A. Giri,²³ P. Goldenzweig,³³ B. Golob,^{43,32} K. Gudkova,^{4,62} C. Hadjivasilou,⁶⁴ T. Hara,^{16,12} O. Hartbrich,¹⁵ H. Hayashii,⁵⁵ M. T. Hedges,¹⁵ M. Hernandez Villanueva,⁴⁹ W.-S. Hou,⁵⁸ C.-L. Hsu,⁷⁶ T. Iijima,^{53,52} K. Inami,⁵² A. Ishikawa,^{16,12} R. Itoh,^{16,12} M. Iwasaki,⁶³ Y. Iwasaki,¹⁶ W. W. Jacobs,²⁵ S. Jia,¹⁰ Y. Jin,⁸⁴ C. W. Joo,³⁴ K. K. Joo,⁶ A. B. Kaliyar,⁷⁸ K. H. Kang,³⁹ G. Karyan,⁸ H. Kichimi,¹⁶ C. Kiesling,⁴⁷ C. H. Kim,¹⁴ D. Y. Kim,⁷⁴ Y.-K. Kim,⁸⁹ K. Kinoshita,⁷ P. Kodyš,⁵ S. Korpar,^{46,32} D. Kotchetkov,¹⁵ P. Krizan,^{43,32} R. Kroeger,⁴⁹ P. Krokovny,^{4,62} R. Kulasiri,³⁵ R. Kumar,⁶⁷ K. Kumara,⁸⁷ Y.-J. Kwon,⁸⁹ J. S. Lange,¹¹ S. C. Lee,³⁹ P. Lewis,² C. H. Li,⁴² L. K. Li,⁷ L. Li Gioi,⁴⁷ J. Libby,²⁴ K. Lieret,⁴⁴ Z. Liptak,^{15,*} D. Liventsev,^{87,16} M. Masuda,^{83,68} T. Matsuda,⁵⁰ M. Merola,^{29,54} F. Metzner,³³ K. Miyabayashi,⁵⁵ H. Miyata,⁶¹ G. B. Mohanty,⁷⁸ S. Mohanty,^{78,85} T. J. Moon,⁷¹ T. Mori,⁵² R. Mussa,³⁰ M. Nakao,^{16,12} H. Nakazawa,⁵⁸ A. Natochii,¹⁵ L. Nayak,²³ M. Nayak,⁸⁰ M. Niiyama,³⁸ N. K. Nisar,³ S. Nishida,^{16,12} K. Ogawa,⁶¹ S. Ogawa,⁸¹ H. Ono,^{60,61} Y. Onuki,⁸⁴ P. Pakhlov,^{41,51} G. Pakhlova,^{18,41} T. Pang,⁶⁶ S. Pardi,²⁹ H. Park,³⁹ S.-H. Park,⁸⁹ S. Paul,^{79,47} T. K. Pedlar,⁴⁵ R. Pestotnik,³² L. E. Piiilonen,⁸⁶ T. Podobnik,^{43,32} V. Popov,¹⁸ E. Prencipe,¹⁹ M. T. Prim,³³ A. Rostomyan,⁸ N. Rout,²⁴ G. Russo,⁵⁴ D. Sahoo,⁷⁸ Y. Sakai,^{16,12} S. Sandilya,^{7,23} A. Sangal,⁷ L. Santelj,^{43,32} T. Sanuki,⁸² V. Savinov,⁶⁶ G. Schnell,^{1,20} J. Schueler,¹⁵ C. Schwanda,²⁷ Y. Seino,⁶¹ K. Senyo,⁸⁸ M. E. Sevir,⁴⁸ M. Shapkin,²⁸ C. P. Shen,¹⁰ J.-G. Shiu,⁵⁸ A. Sokolov,²⁸ E. Solovieva,⁴¹ M. Starič,³² Z. S. Stottler,⁸⁶ K. Sumisawa,^{16,12} M. Takizawa,^{72,17,69} U. Tamponi,³⁰ K. Tanida,³¹ F. Tenchini,⁸ K. Trabelsi,⁴⁰ T. Uglov,^{41,18} Y. Unno,¹⁴ S. Uno,^{16,12} Y. Usov,^{4,62} S. E. Vahsen,¹⁵ R. Van Tonder,² G. Varner,¹⁵ A. Vinokurova,^{4,62} V. Vorobyev,^{4,62,41} E. Waheed,¹⁶ C. H. Wang,⁵⁷ E. Wang,⁶⁶ M.-Z. Wang,⁵⁸ P. Wang,²⁶ M. Watanabe,⁶¹ S. Watanuki,⁴⁰ S. Wehle,⁸ J. Wiechczynski,⁵⁹ E. Won,³⁷ X. Xu,⁷³ B. D. Yabsley,⁷⁶ W. Yan,⁷⁰ S. B. Yang,³⁷ H. Ye,⁸ J. Yelton,⁹ J. H. Yin,³⁷ C. Z. Yuan,²⁶ Y. Yusa,⁶¹ Z. P. Zhang,⁷⁰ V. Zhilich,^{4,62} and V. Zhukova⁴¹

(Belle Collaboration)

¹University of the Basque Country UPV/EHU, 48080 Bilbao

²University of Bonn, 53115 Bonn

³Brookhaven National Laboratory, Upton, New York 11973

⁴Budker Institute of Nuclear Physics SB RAS, Novosibirsk 630090

⁵Faculty of Mathematics and Physics, Charles University, 121 16 Prague

⁶Chonnam National University, Gwangju 61186

⁷University of Cincinnati, Cincinnati, Ohio 45221

⁸Deutsches Elektronen-Synchrotron, 22607 Hamburg

⁹University of Florida, Gainesville, Florida 32611

¹⁰Key Laboratory of Nuclear Physics and Ion-beam Application (MOE) and Institute of Modern Physics, Fudan University, Shanghai 200443

¹¹Justus-Liebig-Universität Gießen, 35392 Gießen

¹²SOKENDAI (The Graduate University for Advanced Studies), Hayama 240-0193

¹³Gyeongsang National University, Jinju 52828

¹⁴Department of Physics and Institute of Natural Sciences, Hanyang University, Seoul 04763

¹⁵University of Hawaii, Honolulu, Hawaii 96822

¹⁶High Energy Accelerator Research Organization (KEK), Tsukuba 305-0801

¹⁷J-PARC Branch, KEK Theory Center, High Energy Accelerator Research Organization (KEK), Tsukuba 305-0801

¹⁸Higher School of Economics (HSE), Moscow 101000

¹⁹Forschungszentrum Jülich, 52425 Jülich

²⁰IKERBASQUE, Basque Foundation for Science, 48013 Bilbao

²¹Indian Institute of Science Education and Research Mohali, SAS Nagar, 140306

²²Indian Institute of Technology Guwahati, Assam 781039

²³Indian Institute of Technology Hyderabad, Telangana 502285

- ²⁴Indian Institute of Technology Madras, Chennai 600036
²⁵Indiana University, Bloomington, Indiana 47408
²⁶Institute of High Energy Physics, Chinese Academy of Sciences, Beijing 100049
²⁷Institute of High Energy Physics, Vienna 1050
²⁸Institute for High Energy Physics, Protvino 142281
²⁹INFN—Sezione di Napoli, 80126 Napoli
³⁰INFN—Sezione di Torino, 10125 Torino
³¹Advanced Science Research Center, Japan Atomic Energy Agency, Naka 319-1195
³²J. Stefan Institute, 1000 Ljubljana
³³Institut für Experimentelle Teilchenphysik, Karlsruher Institut für Technologie, 76131 Karlsruhe
³⁴Kavli Institute for the Physics and Mathematics of the Universe (WPI),
University of Tokyo, Kashiwa 277-8583
³⁵Kennesaw State University, Kennesaw, Georgia 30144
³⁶Korea Institute of Science and Technology Information, Daejeon 34141
³⁷Korea University, Seoul 02841
³⁸Kyoto Sangyo University, Kyoto 603-8555
³⁹Kyungpook National University, Daegu 41566
⁴⁰Université Paris-Saclay, CNRS/IN2P3, IJCLab, 91405 Orsay
⁴¹P.N. Lebedev Physical Institute of the Russian Academy of Sciences, Moscow 119991
⁴²Liaoning Normal University, Dalian 116029
⁴³Faculty of Mathematics and Physics, University of Ljubljana, 1000 Ljubljana
⁴⁴Ludwig Maximilians University, 80539 Munich
⁴⁵Luther College, Decorah, Iowa 52101
⁴⁶University of Maribor, 2000 Maribor
⁴⁷Max-Planck-Institut für Physik, 80805 München
⁴⁸School of Physics, University of Melbourne, Victoria 3010
⁴⁹University of Mississippi, University, Mississippi 38677
⁵⁰University of Miyazaki, Miyazaki 889-2192
⁵¹Moscow Physical Engineering Institute, Moscow 115409
⁵²Graduate School of Science, Nagoya University, Nagoya 464-8602
⁵³Kobayashi-Maskawa Institute, Nagoya University, Nagoya 464-8602
⁵⁴Università di Napoli Federico II, 80126 Napoli
⁵⁵Nara Women's University, Nara 630-8506
⁵⁶National Central University, Chung-li 32054
⁵⁷National United University, Miao Li 36003
⁵⁸Department of Physics, National Taiwan University, Taipei 10617
⁵⁹H. Niewodniczanski Institute of Nuclear Physics, Krakow 31-342
⁶⁰Nippon Dental University, Niigata 951-8580
⁶¹Niigata University, Niigata 950-2181
⁶²Novosibirsk State University, Novosibirsk 630090
⁶³Osaka City University, Osaka 558-8585
⁶⁴Pacific Northwest National Laboratory, Richland, Washington 99352
⁶⁵Panjab University, Chandigarh 160014
⁶⁶University of Pittsburgh, Pittsburgh, Pennsylvania 15260
⁶⁷Punjab Agricultural University, Ludhiana 141004
⁶⁸Research Center for Nuclear Physics, Osaka University, Osaka 567-0047
⁶⁹Meson Science Laboratory, Cluster for Pioneering Research, RIKEN, Saitama 351-0198
⁷⁰Department of Modern Physics and State Key Laboratory of Particle Detection and Electronics,
University of Science and Technology of China, Hefei 230026
⁷¹Seoul National University, Seoul 08826
⁷²Showa Pharmaceutical University, Tokyo 194-8543
⁷³Soochow University, Suzhou 215006
⁷⁴Soongsil University, Seoul 06978
⁷⁵Sungkyunkwan University, Suwon 16419
⁷⁶School of Physics, University of Sydney, New South Wales 2006
⁷⁷Department of Physics, Faculty of Science, University of Tabuk, Tabuk 71451
⁷⁸Tata Institute of Fundamental Research, Mumbai 400005
⁷⁹Department of Physics, Technische Universität München, 85748 Garching
⁸⁰School of Physics and Astronomy, Tel Aviv University, Tel Aviv 69978
⁸¹Toho University, Funabashi 274-8510

⁸²*Department of Physics, Tohoku University, Sendai 980-8578*⁸³*Earthquake Research Institute, University of Tokyo, Tokyo 113-0032*⁸⁴*Department of Physics, University of Tokyo, Tokyo 113-0033*⁸⁵*Utkal University, Bhubaneswar 751004*⁸⁶*Virginia Polytechnic Institute and State University, Blacksburg, Virginia 24061*⁸⁷*Wayne State University, Detroit, Michigan 48202*⁸⁸*Yamagata University, Yamagata 990-8560*⁸⁹*Yonsei University, Seoul 03722* (Received 25 September 2020; accepted 23 October 2020; published 30 November 2020)

Using data collected in the Belle experiment at the KEKB asymmetric-energy e^+e^- collider we search for transitions $\Upsilon(4S) \rightarrow \eta_b(1S)\omega$, $\Upsilon(5S) \rightarrow \eta_b(1S)\omega$ and $\Upsilon(5S) \rightarrow \eta_b(2S)\omega$. No significant signals are observed and we set 90% confidence level upper limits on the corresponding visible cross sections: 0.2 pb, 0.4 pb and 1.9 pb, respectively.

DOI: [10.1103/PhysRevD.102.092011](https://doi.org/10.1103/PhysRevD.102.092011)

I. INTRODUCTION

Recently Belle observed the $\Upsilon(4S) \rightarrow h_b(1P)\eta$ transition and measured its branching fraction to be $\mathcal{B}[\Upsilon(4S) \rightarrow h_b(1P)\eta] = (2.18 \pm 0.21) \times 10^{-3}$ [1]. This value is unexpectedly large in comparison with branching fractions of the $\Upsilon(4S) \rightarrow \Upsilon(1S, 2S)\pi^+\pi^-$ decays [2–4], and represents a strong violation of the heavy quark spin symmetry (HQSS) [5]. A possible mechanism for the HQSS breaking is an admixture of $B\bar{B}$ pairs in the $\Upsilon(4S)$ state [6]. Indeed, the $B\bar{B}$ pair is not an eigenstate of the b quark spin and contains $b\bar{b}$ quarks in both spin-triplet and spin-singlet states. The $\Upsilon(4S) \rightarrow h_b(1P)\eta$ transition proceeds via the spin-singlet component. The transition $\Upsilon(4S) \rightarrow \eta_b(1S)\omega$ might also proceed via the spin-singlet component and thus could be enhanced [6]. Here we perform a search for the $\Upsilon(4S) \rightarrow \eta_b(1S)\omega$ as well as $\Upsilon(10860) \rightarrow \eta_b(1S)\omega$ and $\Upsilon(10860) \rightarrow \eta_b(2S)\omega$ transitions. For brevity, the $\Upsilon(10860)$ state is denoted as $\Upsilon(5S)$ according to its quark model assignment.

We use the full data samples of 711 fb^{-1} and 121 fb^{-1} collected at the $\Upsilon(4S)$ and $\Upsilon(5S)$ resonances by the Belle detector [7] at the KEKB asymmetric-energy e^+e^- collider [8]. The average center-of-mass (c.m.) energy of the $\Upsilon(10860)$ sample is $\sqrt{s} = 10.867 \text{ GeV}$. The Belle detector is a large-solid-angle magnetic spectrometer that consists of a silicon vertex detector, a 50-layer central drift chamber, an array of aerogel threshold Cherenkov counters, a barrel-like arrangement of time-of-flight scintillation counters, and an electromagnetic calorimeter comprised of CsI(Tl) crystals

*Present address: Hiroshima University, Hiroshima 739-8527.

Published by the American Physical Society under the terms of the [Creative Commons Attribution 4.0 International license](https://creativecommons.org/licenses/by/4.0/). Further distribution of this work must maintain attribution to the author(s) and the published article's title, journal citation, and DOI. Funded by SCOAP³.

(ECL) located inside a superconducting solenoid coil that provides a 1.5 T magnetic field. An iron flux-return located outside of the coil is instrumented to detect K_L^0 mesons and to identify muons.

For the Monte Carlo (MC) simulation, we use EvtGen [9] VectorISR model, which correctly describes the angular distribution of ISR photons but uses a flat distribution in photon-energy radiator function. We apply corrections on the ISR photon energy according to Ref. [10]. We use the GEANT3 [11] package to simulate the detector response.

II. EVENT SELECTION

Since the $\eta_b(1S, 2S)$ mesons do not have decay channels that are convenient to reconstruct, we reconstruct only $\omega \rightarrow \pi^+\pi^-\pi^0$ and use the recoil mass $M_{\text{recoil}}(\omega) = \sqrt{(\sqrt{s} - E_\omega^*)^2 - (p_\omega^*)^2}$ to identify the signal, where E_ω^* and p_ω^* are the energy and momentum of the ω meson in the c.m. frame.

We use a generic hadronic event selection with requirements on the position of the primary vertex, track multiplicity, and the total energy and momentum of the event [12]. For charged pions we require the distance of closest approach to the interaction point to be within 2 cm along the beam direction and within 0.2 cm in the plane transverse to the beam direction. We apply loose particle identification requirements to separate charged pions from kaons, protons and electrons. The energy of a photon in the laboratory frame is required to be greater than 50 MeV for the barrel part of the ECL and greater than 100 MeV for the endcap part of the ECL. To further suppress the background from low-energy photons, we require the momentum of the π^0 in the c.m. frame to be above 240 MeV/c, 270 MeV/c and 140 MeV/c for the $\Upsilon(4S) \rightarrow \eta_b(1S)\omega$, $\Upsilon(5S) \rightarrow \eta_b(1S)\omega$ and $\Upsilon(5S) \rightarrow \eta_b(2S)\omega$ transitions, respectively. The masses of the π^0 and ω candidates should satisfy $|M(\gamma\gamma) - m_{\pi^0}| < 8 \text{ MeV}/c^2$ and

$|M(\pi^+\pi^-\pi^0) - m_\omega| < 12 \text{ MeV}/c^2$ [13]. The resolutions in $M(\gamma\gamma)$ and $M(\pi^+\pi^-\pi^0)$ are $5.5 \text{ MeV}/c^2$ and $8 \text{ MeV}/c^2$, respectively.

The $\omega \rightarrow \pi^+\pi^-\pi^0$ events predominantly populate the central part of the Dalitz plot (DP), while background events populate the region near the boundaries. Therefore we require the normalized distance from the DP center, r , to be lower than 0.84. The variable r takes values from $r = 0$ at the DP center to $r = 1$ at its boundary [14].

To suppress background from continuum events $e^+e^- \rightarrow q\bar{q}$ ($q = u, d, s, c$) that have a jetlike shape, we use the angle θ_{thrust} between the thrust axis of $\pi^+\pi^-\pi^0$ and the thrust axis of the rest of the event in the η_b -meson candidate rest frame. The thrust axis is defined as the unit vector \vec{n}_T , which maximizes the thrust value: $T = \sum_i |\vec{p}_i \cdot \vec{n}_T| / \sum_i |\vec{p}_i|$. From the MC simulation we find that the distributions in $\cos(\theta_{\text{thrust}})$ for the signal transitions are uniform; this is because there is no favored direction in the η_b rest frame as its spin is zero. The selection criteria are $|\cos(\theta_{\text{thrust}})| < 0.90$ and $|\cos(\theta_{\text{thrust}})| < 0.70$ for the $\Upsilon(4S) \rightarrow \eta_b(1S)\omega$ and $\Upsilon(5S) \rightarrow \eta_b(1S)\omega$ transitions, respectively, while for the $\Upsilon(5S) \rightarrow \eta_b(2S)\omega$ transition no criteria on $\cos(\theta_{\text{thrust}})$ are applied.

The selection requirements described above are optimized using a figure of merit $N_{\text{sig}}/\sqrt{N_{\text{bkg}}}$, where the signal yield is estimated using MC simulation, and the background yield is estimated using the signal region in data, assuming the signal fraction is very small. For optimization of various requirements we use an iterative procedure. The $M_{\text{recoil}}(\pi^+\pi^-\pi^0)$ is required to be in the interval (9.20, 9.60) GeV/c^2 for the $\eta_b(1S)$ candidates and (9.90, 10.05) GeV/c^2 for the $\eta_b(2S)$ candidates. These intervals are used in the fits described below.

The $M(\pi^+\pi^-\pi^0)$ distribution for the $\Upsilon(4S) \rightarrow \eta_b(1S)\omega$ candidates without the ω mass requirement is shown in Fig. 1. One can see clear signals of the η and ω mesons. The purity of the ω -meson signal is estimated to be 13%. In

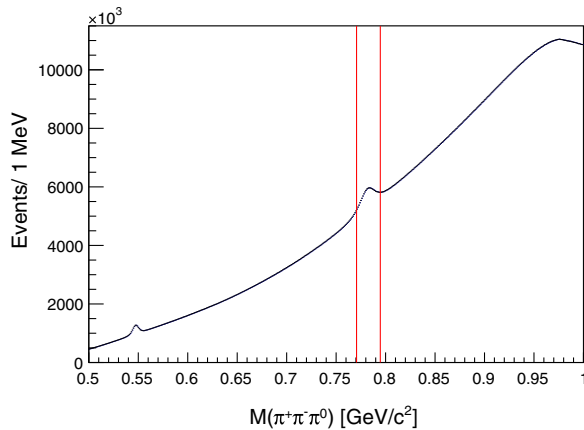


FIG. 1. The $M(\pi^+\pi^-\pi^0)$ distribution for the $\Upsilon(4S) \rightarrow \eta_b(1S)\omega$ candidates. Red lines indicate the ω mass requirement.

the $\Upsilon(5S) \rightarrow \eta_b(1S)\omega$ and $\Upsilon(5S) \rightarrow \eta_b(2S)\omega$ transitions the purities are 24% and 6%, respectively.

We find on average 1.33, 1.12 and 1.63 candidates per event for the $\Upsilon(4S) \rightarrow \eta_b(1S)\omega$, $\Upsilon(5S) \rightarrow \eta_b(1S)\omega$ and $\Upsilon(5S) \rightarrow \eta_b(2S)\omega$ transitions, respectively. The multiple candidates are not correlated in $M_{\text{recoil}}(\pi^+\pi^-\pi^0)$, therefore we do not perform a best candidate selection. The total selection efficiencies are 5.5%, 5.6% and 6.6% for the three transitions, respectively.

III. FIT TO DATA

We perform a binned χ^2 fit to the $M_{\text{recoil}}(\pi^+\pi^-\pi^0)$ distributions in the $\eta_b(1S)$ and $\eta_b(2S)$ mass regions. The fit function is a sum of signal and background components. The signal component is described with a two-sided Crystal Ball (CB) function, which consists of a Gaussian core portion and power-law tails; the function and its first derivative are both continuous [15]. The parameters of the CB function are fixed using MC simulation; the σ -parameters of the core Gaussian are 12.7 MeV/c^2 , 14.6 MeV/c^2 and 9.2 MeV/c^2 for $\Upsilon(4S) \rightarrow \eta_b(1S)\omega$, $\Upsilon(5S) \rightarrow \eta_b(1S)\omega$ and $\Upsilon(5S) \rightarrow \eta_b(2S)\omega$, respectively. The integral of the signal function over the fit range is taken as a signal yield. The background component is described with a Chebyshev polynomial; its order is chosen as the one that gives the maximum p -value for the fit. The polynomial orders are 8, 5 and 6 for the three transitions, respectively. The

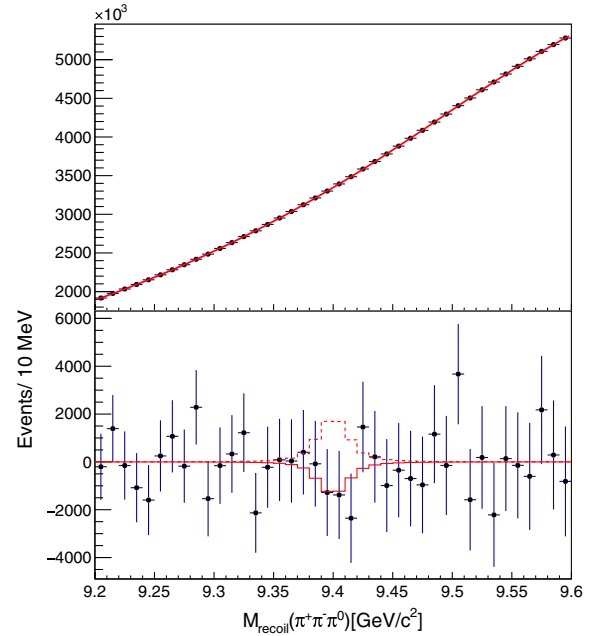


FIG. 2. The $M_{\text{recoil}}(\pi^+\pi^-\pi^0)$ distribution for the $\Upsilon(4S) \rightarrow \eta_b(1S)\omega$ candidates. Top: data points with the fit function overlaid; note the suppressed zero on the vertical scale. Bottom: residuals between the data and the fit function. The solid line shows the fit function for the best fit; the dashed line shows the same function with the yield fixed to the upper limit.

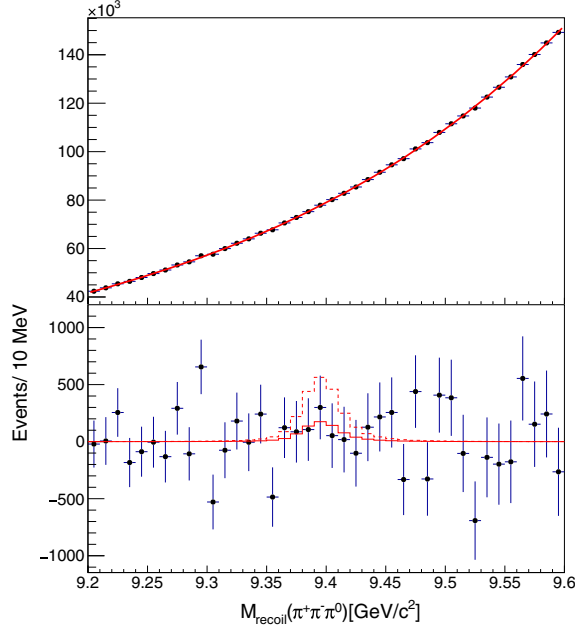


FIG. 3. The $M_{\text{recoil}}(\pi^+\pi^-\pi^0)$ distribution for the $\Upsilon(5S) \rightarrow \eta_b(1S)\omega$ candidates; note the suppressed zero on the vertical scale. Symbols are the same as those in Fig. 2.

$M_{\text{recoil}}(\pi^+\pi^-\pi^0)$ distributions and fit results for $\Upsilon(4S) \rightarrow \eta_b(1S)\omega$, $\Upsilon(5S) \rightarrow \eta_b(1S)\omega$ and $\Upsilon(5S) \rightarrow \eta_b(2S)\omega$ are shown in Figs. 2–4, respectively. We use 1 MeV bins for fitting and 10 MeV bins for visualization to improve clarity. No significant signals are observed. The obtained signal yields for each transition are presented in Table I.

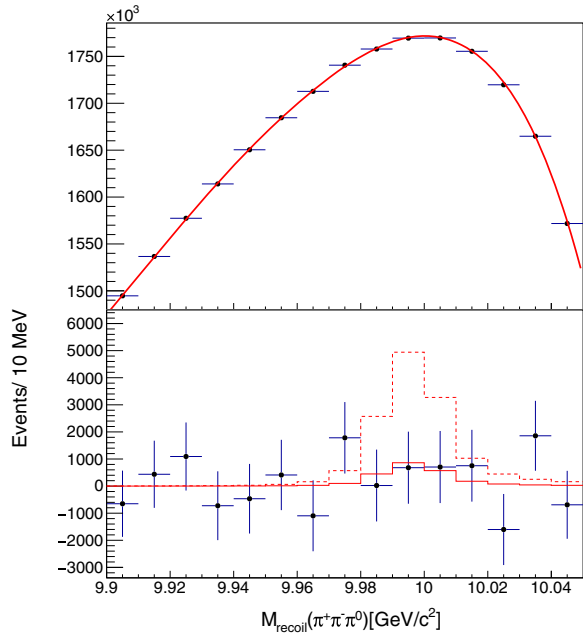


FIG. 4. The $M_{\text{recoil}}(\pi^+\pi^-\pi^0)$ distribution for the $\Upsilon(5S) \rightarrow \eta_b(2S)\omega$ candidates; note the suppressed zero on the vertical scale. Symbols are the same as those in Fig. 2.

TABLE I. Signal yields for various transitions obtained from the fits in units of 10^3 .

$\Upsilon(4S) \rightarrow \eta_b(1S)\omega$	$\Upsilon(5S) \rightarrow \eta_b(1S)\omega$	$\Upsilon(5S) \rightarrow \eta_b(2S)\omega$
$-5.0 \pm 6.6^{+1.5}_{-2.3}$	$0.8 \pm 1.0^{+0.3}_{-0.1}$	$2.4 \pm 5.8^{+3.2}_{-10.8}$

TABLE II. Systematic uncertainties in the yields of various transitions in units of 10^2 .

	$\Upsilon(4S) \rightarrow$		$\Upsilon(5S) \rightarrow$	
	$\eta_b(1S)\omega$	$\eta_b(1S)\omega$	$\eta_b(1S)\omega$	$\eta_b(2S)\omega$
η_b mass	+6	± 0	+27	-34
η_b width	+6	± 1	+5	-4
ISR tail	+0	+2	+2	-0
Background	-12	-0	-0	-0
	+11	+3	+17	+17
	-17	-1	-102	-102
Total	+15	+3	+32	+32
	-23	-1	-108	-108

To set upper limits on the branching fractions, we study the systematic uncertainties in the yields. We vary the $\eta_b(1S)$ and $\eta_b(2S)$ masses and widths within one standard deviation [13]. The $\eta_b(2S)$ width is estimated using a model-independent relation [16]:

$$\begin{aligned} \Gamma[\eta_b(2S)] &= \Gamma[\eta_b(1S)] \cdot \frac{\Gamma[\Upsilon(2S) \rightarrow e^+e^-]}{\Gamma[\Upsilon(1S) \rightarrow e^+e^-]} \\ &= 4.6^{+2.3}_{-1.8} \text{ MeV}. \end{aligned} \quad (1)$$

The ISR tails are sensitive to the energy dependence of the $e^+e^- \rightarrow \eta_b(nS)\omega$ cross sections. Instead of a resonant production via $\Upsilon(4S)$ or $\Upsilon(5S)$, we consider also the cross sections that are energy independent. We generate MC samples for each modification and use them to determine signal shapes. To estimate the uncertainties due to background parametrization we vary the fit range and increase or decrease the polynomial order by one. Maximal deviations in each case are considered to be a systematic uncertainty. The summary of the uncertainties in the yields is presented in Table II. The total systematic uncertainty in the yield is found by adding various contributions in quadrature.

IV. UPPER LIMITS ON VISIBLE CROSS SECTIONS AND BRANCHING FRACTIONS

The visible cross sections are calculated as:

$$\sigma_{\text{vis}}[e^+e^- \rightarrow \eta_b(mS)\omega] = \frac{N}{\epsilon \cdot \mathcal{B}[\omega \rightarrow \pi^+\pi^-\pi^0] \cdot L_{\Upsilon(nS)}}, \quad (2)$$

where $n = 4, 5$ and $m = 1, 2$; N is the signal yield, ϵ is the selection efficiency, $L_{\Upsilon(nS)}$ is the integrated luminosity, $L_{\Upsilon(4S)} = 711 \text{ fb}^{-1}$ and $L_{\Upsilon(5S)} = 121.4 \text{ fb}^{-1}$.

TABLE III. Visible cross sections and upper limits at the 90% confidence level in pb.

	Visible cross section	Upper limit
$e^+e^- \rightarrow \eta_b(1S)\omega$ at $\Upsilon(4S)$	$-0.14^{+0.19}_{-0.20}$	0.2
$e^+e^- \rightarrow \eta_b(1S)\omega$ at $\Upsilon(5S)$	$0.13^{+0.18}_{-0.17}$	0.4
$e^+e^- \rightarrow \eta_b(2S)\omega$ at $\Upsilon(5S)$	$0.3^{+0.9}_{-1.7}$	1.9

We take into account the uncertainty in the efficiency due to possible discrepancies between data and MC simulation (1% per track and 2.2% for π^0), the uncertainty in $\mathcal{B}[\omega \rightarrow \pi^+\pi^-\pi^0]$ [13] and the uncertainty in the $\Upsilon(4S)$ and $\Upsilon(5S)$ integrated luminosity. The total multiplicative uncertainty in the visible cross section is 4.5%.

To combine the uncertainty in the yield, δ_N , which is obtained by adding corresponding statistical and systematic uncertainties in quadrature, and the multiplicative uncertainty δ , we use formula:

$$(N \pm \delta_N) \cdot (1 \pm \delta) = N \pm (\delta_N \oplus N\delta \oplus \delta_N\delta), \quad (3)$$

where the symbol \oplus denotes addition in quadrature.

Estimated visible cross sections and upper limits set using the Feldman-Cousins method [17] at the 90% confidence level are presented in Table III.

We also estimate branching fractions of the $\Upsilon(4S) \rightarrow \eta_b(1S)\omega$, $\Upsilon(5S) \rightarrow \eta_b(1S)\omega$ and $\Upsilon(5S) \rightarrow \eta_b(2S)\omega$ transitions using the number of $\Upsilon(4S)$ or $\Upsilon(5S)$ instead of the luminosity in the denominator of Eq. (2). The number of $\Upsilon(4S)$ is $(771.6 \pm 10.6) \times 10^6$, while the number of $\Upsilon(5S)$ is estimated as $L_{\Upsilon(5S)} \cdot \sigma_{b\bar{b}}$, where $\sigma_{b\bar{b}} = (0.340 \pm 0.016)$ nb [18]. The total multiplicative uncertainty in the branching fraction is 4.5% and 6.5% for transitions from $\Upsilon(4S)$ and $\Upsilon(5S)$, respectively. Estimated branching fractions and upper limits at the 90% confidence level are presented in Table IV.

We also set the upper limit on the ratio:

$$\frac{\mathcal{B}[\Upsilon(4S) \rightarrow \eta_b(1S)\omega]}{\mathcal{B}[\Upsilon(4S) \rightarrow h_b(1P)\eta]} < 8.4 \times 10^{-2} \quad (4)$$

at the 90% confidence level.

V. CROSS-CHECK WITH $\Upsilon(5S) \rightarrow \chi_{bJ}(1P)\omega$

As a cross-check, we perform a search for the $\Upsilon(5S) \rightarrow \chi_{bJ}(1P)\omega$ transitions that were observed previously using

TABLE IV. Branching fractions and upper limits at the 90% confidence level.

	Branching fraction	Upper limit
$\Upsilon(4S) \rightarrow \eta_b(1S)\omega$	$(-1.3^{+1.8}_{-1.9}) \times 10^{-4}$	1.8×10^{-4}
$\Upsilon(5S) \rightarrow \eta_b(1S)\omega$	$(3.7^{+5.4}_{-5.1}) \times 10^{-4}$	1.3×10^{-3}
$\Upsilon(5S) \rightarrow \eta_b(2S)\omega$	$(1.0^{+2.7}_{-5.1}) \times 10^{-3}$	5.6×10^{-3}

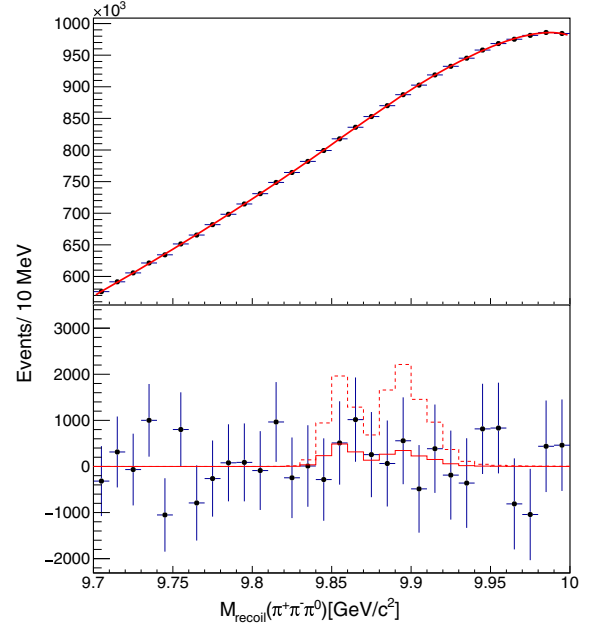


FIG. 5. The $M_{\text{recoil}}(\pi^+\pi^-\pi^0)$ distribution for the $\Upsilon(5S) \rightarrow \chi_{bJ}(1P)\omega$ candidates; note the suppressed zero on the vertical scale. Symbols are the same as those in Fig. 2.

exclusive reconstruction [19]. The analysis procedure is the same as for the $\eta_b(nS)\omega$ transitions. To fit the signal region we use the sum of three CB functions corresponding to $\chi_{b0}(1P)$, $\chi_{b1}(1P)$ and $\chi_{b2}(1P)$ signals. Since we do not have enough resolution to measure $\chi_{b1}(1P)$ and $\chi_{b2}(1P)$ yields individually, we fix the ratio between them according to the known values [19]. To fit the background contribution we use a ninth-order Chebyshev polynomial. The fit result is shown in Fig. 5.

There are no significant signals. The obtained upper limits on branching fractions at the 90% confidence level are

$$\begin{aligned} \mathcal{B}[\Upsilon(5S) \rightarrow \chi_{b0}(1P)\omega] &< 3.0 \times 10^{-3}, \\ \mathcal{B}[\Upsilon(5S) \rightarrow \chi_{b1}(1P)\omega] &< 3.2 \times 10^{-3}. \end{aligned} \quad (5)$$

Since the ratio between $\chi_{b1}(1P)$ and $\chi_{b2}(1P)$ is fixed, we do not give an upper limit for $\chi_{b2}(1P)$. The obtained upper limits are consistent with the exclusive measurement [19]:

$$\begin{aligned} \mathcal{B}[\Upsilon(5S) \rightarrow \chi_{b0}(1P)\omega] &< 3.9 \times 10^{-3}, \\ \mathcal{B}[\Upsilon(5S) \rightarrow \chi_{b1}(1P)\omega] &= (1.57 \pm 0.30) \times 10^{-3}. \end{aligned} \quad (6)$$

VI. CONCLUSION

In summary, we perform a search for the transitions $\Upsilon(4S) \rightarrow \eta_b(1S)\omega$, $\Upsilon(5S) \rightarrow \eta_b(1S)\omega$ and $\Upsilon(5S) \rightarrow \eta_b(2S)\omega$. No significant signals are observed and we set upper limits on visible cross sections and branching fractions presented in Tables III and IV. The upper limit for $\Upsilon(4S) \rightarrow \eta_b(1S)\omega$ is order of magnitude lower than

the value for the similar transition to a spin-singlet state, $\Upsilon(4S) \rightarrow h_b(1P)\eta$ [1]. We set the upper limit on the ratio:

$$\frac{\mathcal{B}[\Upsilon(4S) \rightarrow \eta_b(1S)\omega]}{\mathcal{B}[\Upsilon(4S) \rightarrow h_b(1P)\eta]} < 8.4 \times 10^{-2} \quad (7)$$

at the 90% confidence level. As both transitions are expected to proceed via the $B\bar{B}$ admixture in the $\Upsilon(4S)$ state [6], our result will help to better understand this mechanism. The suppression of the $\Upsilon(4S) \rightarrow \eta_b(1S)\omega$ transition relative to the $\Upsilon(4S) \rightarrow h_b(1P)\eta$ one could be due to different overlaps between the initial state and the bottomonium in the final state or the details of the η and ω meson production.

ACKNOWLEDGMENTS

We thank the KEKB group for the excellent operation of the accelerator; the KEK cryogenics group for the efficient operation of the solenoid; and the KEK computer group, and the Pacific Northwest National Laboratory (PNNL) Environmental Molecular Sciences Laboratory (EMSL) computing group for strong computing support; and the National Institute of Informatics, and Science Information NETwork 5 (SINET5) for valuable network support. We acknowledge support from the Ministry of Education, Culture, Sports, Science, and Technology (MEXT) of Japan, the Japan Society for the Promotion of Science (JSPS), and the Tau-Lepton Physics Research Center of Nagoya University; the Australian Research Council including Grants No. DP-180102629, No. DP170102389, No. DP170102204, No. DP150103061, and No. FT130100303; Austrian Science Fund (FWF); the National Natural Science

Foundation of China under Contracts No. 11435013, No. 11475187, No. 11521505, No. 11575017, No. 11675166, and No. 11705209; Key Research Program of Frontier Sciences, Chinese Academy of Sciences (CAS), Grant No. QYZDJ-SSW-SLH011; the CAS Center for Excellence in Particle Physics (CCEPP); the Shanghai Pujiang Program under Grant No. 18PJ1401000; the Ministry of Education, Youth and Sports of the Czech Republic under Contract No. LTT17020; the Carl Zeiss Foundation, the Deutsche Forschungsgemeinschaft, the Excellence Cluster Universe, and the VolkswagenStiftung; the Department of Science and Technology of India; the Istituto Nazionale di Fisica Nucleare of Italy; National Research Foundation (NRF) of Korea Grants No. 2016-R1D1A1B01010135, No. 2016R1D1A1B02012900, No. 2018R1A2B3003643, No. 2018R1A6A1A06024970, No. 2018R1D1A1B07047294, No. 2019K1A3A7A-09033840, and No. 2019R1I1A3A01058933; Radiation Science Research Institute, Foreign Large-size Research Facility Application Supporting project, the Global Science Experimental Data Hub Center of the Korea Institute of Science and Technology Information and KREONET/GLORIAD; the Polish Ministry of Science and Higher Education and the National Science Center; the Russian Science Foundation (RSF), Grant No. 18-12-00226; University of Tabuk research Grants No. S-0256-1438 and No. S-0280-1439 (Saudi Arabia); the Slovenian Research Agency; Ikerbasque, Basque Foundation for Science, Spain; the Swiss National Science Foundation; the Ministry of Education and the Ministry of Science and Technology of Taiwan; and the United States Department of Energy and the National Science Foundation.

-
- [1] U. Tamponi *et al.* (Belle Collaboration), First observation of the hadronic transition $\Upsilon(4S) \rightarrow \eta h_b(1P)$ and new measurement of the $h_b(1P)$ and $\eta_b(1S)$ parameters, *Phys. Rev. Lett.* **115**, 142001 (2015).
- [2] E. Guido *et al.* (Belle Collaboration), Study of η and dipion transitions in $\Upsilon(4S)$ decays to lower bottomonia, *Phys. Rev. D* **96**, 052005 (2017).
- [3] B. Aubert *et al.* (BABAR Collaboration), Study of hadronic transitions between Upsilon states and observation of $\Upsilon(4S) \rightarrow \eta\Upsilon(1S)$ decay, *Phys. Rev. D* **78**, 112002 (2008).
- [4] I. Adachi *et al.* (Belle Collaboration), First observation of the P -wave spin-singlet bottomonium states $h_b(1P)$ and $h_b(2P)$, *Phys. Rev. Lett.* **108**, 032001 (2012).
- [5] A. E. Bondar, R. V. Mizuk, and M. B. Voloshin, Bottomonium-like states: Physics case for energy scan above the $B\bar{B}$ threshold at Belle-II, *Mod. Phys. Lett. A* **32**, 1750025 (2017).
- [6] M. B. Voloshin, Heavy quark spin symmetry breaking in near-threshold $J^{PC} = 1^{--}$ quarkonium-like resonances, *Phys. Rev. D* **85**, 034024 (2012).
- [7] A. Abashian *et al.*, The Belle Detector, *Nucl. Instrum. Methods Phys. Res., Sect. A* **479**, 117 (2002).
- [8] S. Kurokawa and E. Kikutani, Overview of the KEKB accelerators, *Nucl. Instrum. Methods Phys. Res., Sect. A* **499**, 1 (2003), and other papers included in this Volume; T. Abe *et al.*, Achievements of KEKB, *Prog. Theor. Exp. Phys.* **2013**, 03A001 (2013), and references therein.
- [9] D. J. Lange, The EvtGen particle decay simulation package, *Nucl. Instrum. Methods Phys. Res., Sect. A* **462**, 152 (2001).
- [10] M. Benayoun, S. I. Eidelman, V. N. Ivanchenko, and Z. K. Silagadze, Spectroscopy at B factories using hard photon emission, *Mod. Phys. Lett. A* **14**, 2605 (1999).
- [11] R. Brun *et al.*, GEANT3.21, CERN Report No. DD/EE/84-1, 1984.
- [12] K. Abe *et al.* (Belle Collaboration), Measurement of inclusive production of neutral pions from Upsilon(4S) decays, *Phys. Rev. D* **64**, 072001 (2001).
- [13] P. A. Zyla *et al.* (Particle Data Group), Particle Data Group, *Prog. Theor. Exp. Phys.* **2020**, 083C01 (2020).

- [14] D. Matvienko *et al.* (Belle Collaboration), Study of D^{**} production and light hadronic states in the $\bar{B}^0 \rightarrow D^{*+} \omega \pi^-$ decay, *Phys. Rev. D* **92**, 012013 (2015).
- [15] T. Skwarnicki, A study of the radiative CASCADE transitions between the Upsilon-Prime and Upsilon resonances, Ph.D. thesis, Institute of Nuclear Physics, Krakow, DESY Report No. DESY-F31-86-02, 1986.
- [16] M. B. Voloshin, Charmonium, *Prog. Part. Nucl. Phys.* **61**, 455 (2008).
- [17] G. J. Feldman and R. D. Cousins, A Unified approach to the classical statistical analysis of small signals, *Phys. Rev. D* **57**, 3873 (1998).
- [18] U. Tamponi *et al.* (Belle Collaboration), Inclusive study of bottomonium production in association with an η meson in e^+e^- annihilations near $\Upsilon(5S)$, *Eur. Phys. J. C* **78**, 633 (2018).
- [19] X. H. He *et al.* (Belle Collaboration), Observation of $e^+e^- \rightarrow \pi^+\pi^-\pi^0\chi_{bJ}$ and Search for $X_b \rightarrow \omega\Upsilon(1S)$ at $\sqrt{s} = 10.867$ GeV, *Phys. Rev. Lett.* **113**, 142001 (2014).